Inorg. Chem. **2002**, *41*, 5744–5753

Metal Substitution in the Active Site of Nitrogenase MFe_7S_9 ($M = Mo^{4+}$, V^{3+}, Fe^{3+})

Timothy Lovell,* Rhonda A. Torres, Wen-Ge Han, Tiqing Liu, David A. Case, and Louis Noodleman*

Department of Molecular Biology TPC-15, The Scripps Research Institute, La Jolla, California 92037

Received July 22, 2002

The unifying view that molybdenum is the essential component in nitrogenase has changed over the past few years with the discovery of a vanadium-containing nitrogenase and an iron-only nitrogenase. The principal question that has arisen for the alternative nitrogenases concerns the structures of their corresponding cofactors and their metal-ion valence assignments and whether there are significant differences with that of the more widely known molybdenum–iron cofactor (FeMoco). Spin-polarized broken-symmetry (BS) density functional theory (DFT) calculations are used to assess which of the two possible metal-ion valence assignments ($4Fe^{2+}4Fe^{3+}$ or $6Fe^{2+}$-$2Fe^{3+}$) for the iron-only cofactor (FeFeco) best represents the resting state. For the $6Fe^{2+}2Fe^{3+}$ oxidation state, the spin coupling pattern for several spin state alignments compatible with $S = 0$ were generated and assessed by energy criteria. The most likely BS spin state is composed of a 4Fe cluster with spin $S_a = {}^7/_2$ antiferromagnetically coupled to a 4Fe′ cluster with spin $S_b = {}^7/_2$. This state has the lowest DFT energy for the isolated FeFeco cluster and displays calculated Mössbauer isomer shifts consistent with experiment. Although the $S = 0$ resting state of FeFeco has recently been proposed to have metal-ion valencies of $4Fe^{2+}4Fe^{3+}$ (derived from experimental Mössbauer isomer shifts), our isomer shift calculations for the $4Fe^{2+}4Fe^{3+}$ oxidation state are in poorer agreement with experiment. Using the $Mo^{4+}6Fe^{2+}Fe^{3+}$ oxidation level of the cofactor as a starting point, the structural consequences of replacement of molybdenum (Mo^{4+}) with vanadium (V^{3+}) or iron (Fe^{3+}) in the cofactor have been investigated. The size of the cofactor cluster shows a dependency on the nature of the heterometal and increases in the order FeMoco < FeVco < FeFeco.

1. Introduction

MoFe nitrogenase, one of three[1] related forms of the metalloprotein system responsible for biological nitrogen fixation,[2] catalyzes the reduction of dinitrogen (N_2) to ammonia (NH_3) under ambient conditions via the reaction

$$N_2 + 8H^+ + 8e^- + 16MgATP \rightarrow 2NH_3 + H_2 + 16MgADP + 16P_i$$

The Mo-based nitrogenase system contains two easily separable protein components, the Fe protein and the MoFe protein, each named according to its metal-containing prosthetic groups. The smaller γ_2 Fe protein contains a single 4Fe4S cluster which serves as the specific MgATP-dependent reductant to the larger $\alpha_2\beta_2$ MoFe protein, where two unique metal-containing clusters exist within each $\alpha\beta$ pair. These two clusters are denoted as the 8Fe P-cluster and the 7FeMo cofactor (FeMoco); the former evidently transfers electrons while the latter is the proposed site of binding and reduction of N_2 and other molecules.

The FeMoco from *Azotobacter vinelandii* is located in the α-subunit of the MoFe protein and is covalently linked to the protein by a cysteine (Cys275) ligated to an Fe atom and a histidine (His442) bound to a Mo atom.[3] *R*-Homocitrate is also bound to Mo to complete its octahedral coordination

* To whom correspondence should be addressed. Email: tlovell@scripps.edu (T.L.); lou@scripps.edu (L.N.). Fax: +1 858 784 8896.

(1) An unrelated superoxide-dependent Mo-containing system isolated from *Streptomyces thermoautotrophicus* has recently been described. Hofmann-Findeklee, C.; Gadkari, D.; Meyer, O. In *Nitrogen Fixation*: *From Molecules to Crop Productivity*; Pedrosa, F. O., Hungria, M., Yates, M. G., Newton, W. E., Eds.; Kluwer Academic Publishers: Dordrecht, The Netherlands, 2000; pp 23−30.

(2) (a) Stacey, G.; Burris, R. H.; Evans, H. J. *Biological Nitrogen Fixation*; Chapman and Hall: New York, 1992. (b) Steifel, E. I.; Concouvanis, D.; Newton, W. E. *Molydenum Enzymes*, *Cofactors*, *and Model Systems*; American Chemical Society: Washington, DC, 1993. (c) Holm, R. H.; Kennepohl, P.; Solomon, E. I. *Chem. Rev.* **1996**, *96*, 2239.

(3) (a) Kim, J.; Rees, D. C. *Nature* **1992**, *360*, 553. (b) Kim, J.; Rees, D. C. *Science* **1992**, *257*, 1677. (c) Chan, M. K.; Kim, J.; Rees, D. C. *Science* **1993**, *260*, 792. (d) Peters, J. W.; Stowell, M. H. B.; Soltis, S. M.; Finnegan, M. G.; Johnson, M. K.; Rees, D. C. *Biochemistry* **1997**, *36*, 1181.

10.1021/ic020474u CCC: $22.00
Published on Web 09/28/2002

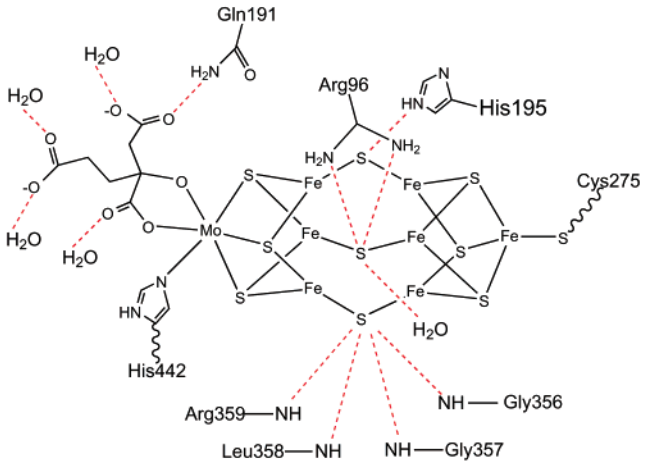

Figure 1. FeMo cofactor located in the α-subunit of the MoFe protein from *A. vinelandii*. Hydrogen bonds to second shell residues and water molecules are shown also.

sphere, and several hydrogen bonds exist between the protein and solvent environment and various sulfur and oxygen sites of the FeMoco (Figure 1). In the resting state, FeMoco has long been known to exhibit an $S = {}^3/_2$ EPR signal.[4] Combined ^{57}Fe Q-band ENDOR and EPR data suggested metal-valence assignments of $1Mo^{4+}6Fe^{2+}1Fe^{3+}$ were appropriate for FeMoco,[5] but an alternative $1Mo^{4+}4Fe^{2+}3Fe^{3+}$ assignment has been proposed from recent Mössbauer experiments. The Mössbauer analysis also indicates the presence of a complicated 4(↑):3(↓) pattern of Fe site spins within the cofactor.[6]

The intriguing discovery that some nitrogenases display a cofactor in which molybdenum is replaced by vanadium or iron has stimulated extensive research into nitrogenase.[7] Unlike its MoFe counterpart, the VFe protein has not yet been characterized by X-ray crystallography, but EXAFS, EPR, and Mössbauer data are available.[8] The $S = {}^3/_2$ signal from the majority species in the EPR in combination with all the other data is suggestive that the metal clusters are structurally homologous to those of the MoFe nitrogenase. However, the specific coupling pattern of Fe site spins that gives rise to the total cluster spin of $S = {}^3/_2$ is not known for FeVco. Given the overall similarities in the EPR signals for the MoFe and VFe proteins and the diagonal relationship that exists between the Mo^{4+} and V^{3+} ions in the periodic table,[9] it has been supposed that the same spin coupling pattern is present in the FeMoco and FeVco clusters.

Structural information on the metal clusters of the iron-only nitrogenase by spectroscopic methods has been even more limited than for the FeVco; however, the EPR and biochemical indications are that the FeFeco is structurally analogous to the FeMoco and FeVco.[10] The most recent K-edge EXAFS data suggest the main three-dimensional elements of the FeMoco, such as the central trigonal prismatic arrangement of the Fe atoms and the covalent links to the protein, are also present in the FeFeco.[11] One noteworthy difference is that the characteristic and readily detectable $S = {}^3/_2$ signal associated with FeMoco and FeVco is no longer present in FeFeco. The absence of an EPR signal assignable to the FeFeco centers in the protein suggests that replacement of Mo or V by Fe results in a significant difference in the spin coupling within the cofactor.

^{57}Fe Mössbauer experiments in the presence of a strong magnetic field further confirm that the iron-only cofactor is diamagnetic,[11] and suggest that from a formal oxidation state sense the replacement of Mo with an Fe atom is not a direct isoelectronic substitution. A requirement of the change in total spin state of the cofactor from $S = {}^3/_2$ (in FeMoco and FeVco) to $S = 0$ (in FeFeco) is that the "introduced" iron maintains a high-spin $Fe^{3+}(d^5)$ electronic configuration and cannot be Fe^{2+}. It is therefore likely that an integer spin ground state for FeFeco (probably $S = 0$) arises from antiferromagnetic coupling of the Fe site spins, but the specific pattern of Fe site spins that gives rise to this state is presently unresolved.

To attain an integer spin ground state, FeFeco must possess an even number of Fe^{2+} and Fe^{3+} sites. Formal oxidation states of $4Fe^{3+}4Fe^{2+}$ have been proposed based primarily on a linear interpolation between the observed Mössbauer isomer shift of the only available synthetic 1Fe complex $([Fe(SR)_3]^{1-}$ (R = 2,4,6-*t*Butyl$_3$C$_6$H$_2$) with a high-spin Fe^{2+} isomer shift of 0.57 mm/s.[12] A similar rationale was also recently applied to the FeMoco in assigning its metal-ion valencies as $Mo^{4+}4Fe^{2+}3Fe^{3+}$ in the resting state.[6] Recent broken-symmetry (BS) density functional theory (DFT) calculations on FeMoco suggest that the linear interpolation procedure from three- and four-coordinate 1Fe complexes does not reliably predict the isomer shifts of the more

(4) (a) Burgess, B. K.; Lowe, D. J. *Chem. Rev.* **1996**, *96*, 2983 and references therein. (b) Ferguson, S. J. *Curr. Opin. Chem. Biol*. **1998**, *2*, 182.
(5) (a) Lee, H.-I.; Hales, B. J.; Hoffman, B. M. *J. Am. Chem. Soc*. **1997**, *119*, 11395. (b) Hoffmann, B. M.; Roberts, J. E.; Orme-Johnson, W. H. *J. Am. Chem. Soc*. **1982**, *104*, 860. (c) Venters, R. A.; Nelson, M. J.; McLean, P. A.; True, A. E.; Levy, M. A.; Hoffmann, B. M. *J. Am. Chem. Soc.* **1986**, *108*, 3487. (d) McLean, P. A.; True, A. E.; Nelson, M. J.; Chapman, S.; Godfrey, M. R.; Teo, B. K.; Orme-Johnson, W. H.; Hoffmann, B. M. *J. Am. Chem. Soc*. **1987**, *109*, 943. (e) True, A. E.; McLean, P.; Nelson, M. J.; Orme-Johnson, W. H.; Hoffmann, B. M. *J. Am. Chem. Soc*. **1990**, *112*, 651.
(6) Yoo, S. J.; Angove, H. C.; Papaefthymiou, V.; Burgess, B. K.; Münck, E. *J. Am. Chem. Soc.* **2000**, *122*, 4926.
(7) Eady, R. R. *Chem. Rev*. **1996**, *96*, 3013.
(8) (a) Chen, J.; Christiansen, J.; Tittsworth, R. J.; Hales, B. J.; George, S. J.; Coucouvanis, D.; Cramer, S. P. *J. Am. Chem. Soc*. **1993**, *115*, 5509. (b) Arber, J. M.; Dobson, B. R.; Eady, R. R.; Hasnain, S. S.; Garner, C. D.; Matsushita, T.; Nomura, M.; Smith, B. E. *Biochem. J.* **1989**, *258*, 733. (c) George, G. N.; Coyle, C. L.; Hales, B. J.; Cramer, S. P. *J. Am. Chem. Soc.* **1988**, *110*, 4057. (d) Harvey, I.; Arber, J. M.; Eady, R. R.; Smith, B. E.; Garner, C. D.; Hasnain, S. S. *Biochem. J.* **1990**, *266*, 929.
(9) Cotton, F. A.; Wilkinson, G. *Advanced Inorganic Chemistry*, 5th ed.; John Wiley: New York, 1988.
(10) (a) Gollan, U.; Schneider, K.; Müller, A.; Schuddekopf, K.; Klipp, W. *Eur. J. Biochem*. **1993**, *215*, 25. (b) Ravi, N.; Moore, V.; Lloyd, S. G.; Hales, B. J.; Huynh, B. H. *J. Biol. Chem*. **1994**, *269*, 20920. (c) Pau, R. N.; Eldridge, M. E.; Lowe, D. J.; Mitchenall, L. A.; Eady, R. R.; *Biochem. J*. **1993**, *293*, 101. (d) Davis, R.; Lehman, L.; Petrovich, R.; Shah, V. K.; Roberts, G. P.; Ludden, P. W. *J. Bacteriol.* **1996**, *178*, 1445. (e) Moore, V. G.; Tittsworth, R. C.; Hales, B. J. *J. Am. Chem. Soc*. **1994**, *116*, 12101. (f) Smith, B. E.; Eady, R. R.; Lowe, D. J.; Gormal, C. *Biochem. J*. **1988**, *250*, 299.
(11) Krahn, E.; Weiss, B. J. R.; Kröckel, M.; Groppe, J.; Henkel, G.; Cramer, S. P.; Trautwein, A. X.; Schneider, K.; Müller, A. *JBIC, J. Biol. Inorg. Chem.* **2002**, *7*, 37.
(12) MacDonnell, F. M.; Rohlandt-Senge, K.; Ellison, J. J.; Holm, R. H.; Power, P. P. *Inorg. Chem*. **1995**, *34*, 1815.

complicated FeMoco cluster.[13] The validity of the assignment for FeFeco is further brought into question especially when one also considers the ENDOR assignments[5] for FeMoco in which the metal-ion valencies were $Mo^{4+}6Fe^{2+}1Fe^{3+}$ and FeMoco, in fact, appears to be two electrons more reduced than that proposed by the Mössbauer data. Therefore, the possibility that the oxidation state assignment in FeFeco may also be two electrons more reduced, i.e., $2Fe^{3+}6Fe^{2+}$, must also be considered.

Theoretical studies provide a platform for comparing and better understanding spin coupling and structural parameters of the nitrogenase factors. Computational studies so far have largely focused on the more extensively characterized FeMoco and understanding the mechanism of MoFe nitrogenase catalysis.[14] Few theoretical studies have been conducted at high enough levels of theory on the FeVco and FeFeco clusters.[15] Our recent calculations[13] on the FeMoco provided a qualitatively correct electronic structure of the cluster, with reasonable estimates of the properties (including the strong antiferromagnetic interaction) of the FeMo cofactor, and lend support to the $Mo^{4+}6Fe^{2+}1Fe^{3+}$ oxidation state assignment. Given that the experimental indications are that FeMoco, FeVco, and FeFeco are isostructural, in this contribution we examine the effect of metal-ion replacement on the structures of active site cofactors of nitrogenase and evaluate whether the postulated structural homology of the cofactors is manifested in the DFT calculations. The possible spin coupling alignments in FeFeco that give rise to a total cluster spin of $S = 0$ are also investigated, and by comparison and contrast with our previous work on FeMoco, the most likely oxidation states of the Fe sites in the FeFeco and for V in the FeVco are suggested.

2. Methods

2.1. Quantum Model of Nitrogenase Cofactors and Immediate Protein Environment. X-ray crystallographic coordinates have been reported for nitrogenase from several bacterial sources.[16] The starting geometry for the cofactor models was based on our optimized FeMoco structure.[13] The original starting geometry was obtained from the 1MIN structure from *Azotobacter vinelandii* (2.2 Å resolution) and later refined using the 2MIN (2.0 Å resolution) structure.[3] The model clusters comprise the [M7Fe9S] ($M = Mo^{4+}$, V^{3+}, Fe^{3+}) cores, the side chain ligands of Cys275 (represented by a methyl thiolate), His442 (represented by an imidazole), and the fully deprotonated homocitrate ligand (charge $= -4$) within the first coordination shell. A number of second shell ligands have also been included in the model: the side chain of Gln191 (represented by acetamide) and four structurally characterized water molecules (Wat639, Wat610, Wat631, and Wat633 from 2MIN[3]) which are the hydrogen-bonding partners to the negatively charged oxygen ends of the homocitrate ligand. Total charges on the cofactor structural models (shown in Figure 2) are -4 for FeMoco and -5 for FeVco and FeFeco.

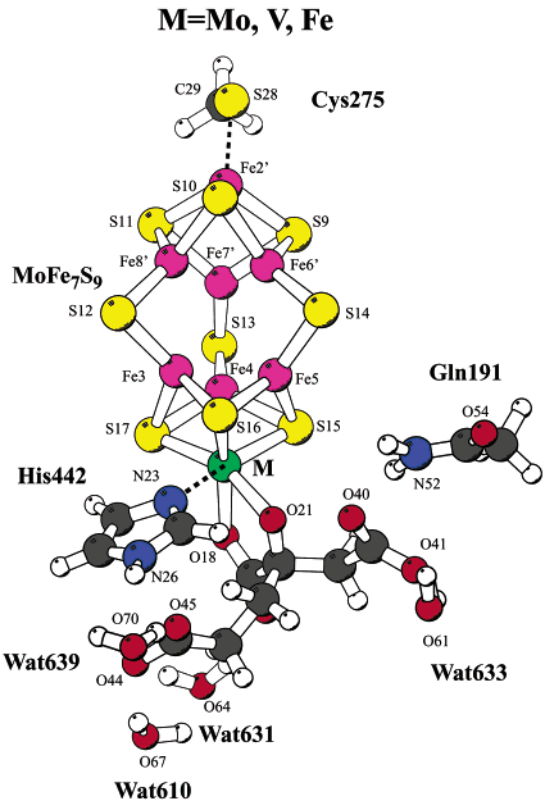

Figure 2. Quantum cluster model of nitrogenase cofactor and surrounding protein environment. Model was constructed on the basis of the FeMo cofactor located in the α-subunit of the MoFe protein from *A. vinelandii*. FeVco and FeFeco clusters were constructed to have similar starting geometries based on the postulated structural homology between the cofactors. Atoms are identified by color: green (heterometal = molybdenum, vanadium, or iron); magenta (iron); yellow (sulfur); red (oxygen); blue (nitrogen); dark gray (carbon). Figure was prepared using MOLSCRIPT: Kraulis, P. J. *J. Appl. Crystallogr.* **1991**, *24*, 946.

2.2. Density Functional Calculations. The Amsterdam Density functional package (ADF, version 2.3)[17] was used to compute the geometries and energies of the active site clusters. The ADF basis set IV was used for all atoms, corresponding to uncontracted triple-ζ Slater-type orbitals (STO) for the 4s, 4p, 5s, and 4d valence orbitals of Mo, 3s, 3p, 4s, and 3d valence orbitals of Fe, 3s, 3p, 4s, and 3d valence orbitals of V, triple-ζ STOs for the 2s, 2p valence orbitals of C, N, O augmented with a 3d polarization orbital, and triple-ζ

(13) Lovell, T.; Li, J.; Liu, T.; Case, D. A.; Noodleman, L. *J. Am. Chem. Soc.* **2001**, *123*, 12392.
(14) (a) Deng, H.; Hoffmann, R. *Angew. Chem., Int. Ed. Engl.* **1993**, *32*, 1062. (b) Stavrev, K. K.; Zerner, M. C. *Chem.—Eur. J.* **1996**, *2*, 83. (c) Stavrev, K. K.; Zerner, M. C. *Theor. Chim. Acta* **1997**, *96*, 141. (d) Stavrev, K. K.; Zerner, M. C. *Int. J. Quantum Chem.* **1998**, *70*, 1159. (e) Dance, I. *Aust. J. Chem.* **1994**, *47*, 979. (f) Dance, I. *Chem. Commun.* **1997**, 165. (g) Dance, I. *Chem. Commun.* **1998**, 523. (h) Dance, I. *JBIC, J. Biol. Inorg. Chem.* **1996**, *1*, 581. (i) Siegbahn, P. E. M.; Westerberg, J.; Svensson, M.; Crabtree, R. H. *J. Phys. Chem. B* **1998**, *102*, 1615. (i) Rod, T. H.; Hammer, B.; Nørskov, J. K. *Phys. Rev. Lett.* **1999**, *82*, 4054. (j) Rod, T. H.; Logadottir, A.; Nørskov, J. K. *J. Chem. Phys.* **2000**, *112*, 5343. (k) Rod, T. H.; Nørskov, J. K. *J. Am. Chem. Soc.* **2000**, *122*, 12751. (l) Szilagyi, R. K.; Musaev, D. K.; Morokuma, K. *Inorg. Chem.* **2001**, *40*, 766.
(15) Plass, W. *THEOCHEM*, **1994**, *315*, 53.
(16) (a) Kim, J.; Rees, D. C. *Nature* **1992**, *360*, 553. (b) Kim, J.; Rees, D. C. *Science* **1992**, *257*, 1677. (c) Chan, M. K.; Kim, J.; Rees, D. C. *Science* **1993**, *260*, 792. (d) Georgiadis, M. M.; Komiya, H.; Woo, D.; Kornuc, J. J.; Rees, D. C. *Science* **1992**, *257*, 1653. (e) Kim, J.; Woo, D.; Rees, D. C. *Biochemistry* **1993**, *32*, 7104. (f) Bolin, J. T.; Ronco, A. E.; Morgan, T. V.; Mortenson, L. E.; Xuong, N. *Proc. Natl. Acad. Sci. U.S.A.* **1993**, *90*, 1078. (g) Mayer, S. M.; Lawson, D. M.; Gormal, C. A.; Roe, S. M.; Smith, B. E. *J. Mol. Biol.* **1999**, *292*, 871. (h) Schindelin, N.; Kisker, C.; Schlessman, J. L.; Howard, J. B.; Rees, D. C. *Nature* **1997**, *387*, 370. (i) Strop, P.; Takahara, P. M.; Chiu, H.-J.; Angove, H. C.; Burgess, B. K.; Rees, D. C. *Biochemistry*, **2001**, *40*, 651.
(17) *ADF 2.3.0*; Department of Theoretical Chemistry, Free University of Amsterdam: Amsterdam, 1997.

STO for 1s of H with a 2p polarization orbital.[18,19] Electrons in orbitals up to and including 3d {Mo}, 2p {V, Fe, S}, and 1s {N, O, C} were considered to be part of the core and treated in accordance with the frozen core approximation. The numerical integration scheme was the polyhedron method developed by the Velde et al.[20] For all geometry optimizations, the analytical gradient method implemented by Versluis et al.[21,22] was used with a numerical integration accuracy of 4.0. Convergence criteria were set to 0.001 Å in coordinates and 0.01 Hartree/Å in the norm of all gradient vectors. The geometry optimizations in this paper were performed using the generalized gradient correction terms included in the SCF potential (local Vosko−Wilk−Nusair (VWN) + nonlocal Becke−Perdew (BP86) for exchange and correlation).[23,24] Calculations were performed without symmetry using a parallel version of the ADF code on four SGI R10000 nodes. Within the M7Fe9S(Cys275·Sγ)(His442·Nδ)2O (M = Mo, Fe, V) core, all bond lengths and angles were fully optimized. With the exception of the atoms directly ligated to the M (M = Mo, Fe, V) and 7Fe centers, the internal geometries (but not the relative positions) of coordinated protein residues within the first sphere, such as the imidazole ring and the methyl component of the methyl thiolate group, were constrained to their X-ray coordinates. Second shell ligands were given all degrees of freedom, allowing for the possible transfer of protons between the unsaturated oxygens of the homocitrate and the second shell hydrogen-bonding ligands (Gln191 and 4 waters) to occur.[25]

To describe spin polarization and spin coupling, the calculations were done with the spin-unrestricted broken-symmetry (BS) approach.[26] The BS state is not a pure spin state, but rather a mixed state in which the majority spin and minority spin are arranged either spin up and spin down to give a spin coupling pattern with the correct net total spin and either an overall antiferromagnetic (AF) or ferromagnetic (F) alignment. The energy of such a BS state is usually above, but close to, the true ground state energy.[27] To construct a desired BS state, a calculation on the high-spin (HS) state is first completed, which is a pure spin state described by a single determinant, with all unpaired electrons aligned in the same direction (spin up) to adopt the highest possible total spin state *S*. For the M6Fe^{2+}1Fe^{3+} oxidation state, the high-spin states have total spin $S = {}^{29}/_{2}$ (M = Mo^{4+}, V^{3+}) and $S = {}^{34}/_{2}$ (M = Fe^{3+}); for M4Fe^{2+}3Fe^{3+}, the corresponding high-spin states are $S = {}^{31}/_{2}$ (M = Mo^{4+}, V^{3+}) and $S = {}^{36}/_{2}$ (M = Fe^{3+}). The density of the HS state is then manipulated by exchanging designated blocks of α and β electron densities (from the fit electron density in ADF). In this way, the starting density for the desired spin-flipped $S = {}^{3}/_{2}$ state (M = Mo^{4+}, V^{3+}) and $S = 0$ (M = Fe^{3+}) is created, from which BS states are obtained by SCF convergence.[28]

3. Results

3.1. Qualitative Spin Coupling in FeMoco and FeVco Clusters. The resting states of the MoFe and VFe nitrogenases exhibit an $S = {}^{3}/_{2}$ EPR signal resulting from the cofactors. Using spin-projection coefficient analysis procedures,[29] Lee et al. have proposed an assignment of the metal-ion valencies from their ^{57}Fe Q-band ENDOR measurements for FeMoco.[5] This proposal of [Mo^{4+}Fe^{3+}6Fe^{2+}9S^{2-}]$^{+}$ gives a formal d-electron count of 43. Assuming high-spin transition metal ions, many possible spin alignment patterns exist which satisfy $S = {}^{3}/_{2}$ and the given metal-ion valencies. With molybdenum assumed to be in the Mo^{4+}(d^2) oxidation state and low spin in the octahedral environment of O, N, and S-based ligands, the $S = {}^{3}/_{2}$ spin state of the cofactor results from spin coupling of one ferric (Fe^{3+}, high-spin d,[5] $S = {}^{5}/_{2}$) and six ferrous ions (Fe^{2+}, high-spin d,[6] $S = 2$). This $S = {}^{3}/_{2}$ spin condition may be satisfied by aligning the Fe site spin vectors as follows:

$$\begin{aligned} M_s(\text{total}) &= M_s(\text{3Fe triangle}) + M_s(\text{4Fe′ cubane}) \\ &= M_s(\text{Fe}_3 + \text{Fe}_4 + \text{Fe}_5) + M_s(\text{Fe}_2' + \text{Fe}_6' + \text{Fe}_7' + \text{Fe}_8') \\ &= (+2 - 2 - 2) + (-{}^{5}/_{2} + 2 + 2 + 2) \\ &= {}^{3}/_{2} \end{aligned} \quad (1)$$

This represents one of a number of possible spin alignments with all spin alignments corresponding to the two M_s(total) = $\pm {}^{3}/_{2}$ values and a 4:3 pattern of majority spin up to majority spin down Fe sites or vice versa.

X-ray absorption spectroscopy has been used to propose the oxidation state of V in FeVco. Features of the absorption edge are indicative of a V^{2+}, V^{3+}, or V^{4+} ion in a distorted octahedral environment.[30,9c] In FeMoco, the very small Mo hyperfine interactions has resulted in molybdenum being

(18) (a) Snijders, J. G.; Baerends, E. J.; Vernooijs, P. *At. Nucl. Data Tables* **1982**, *26*, 483. (b) Vernooijs, P.; Snijders, J. G.; Baerends, E. J. *Slater Type Basis Functions for the Whole Periodic System*; Internal report; Free University of Amsterdam: Amsterdam, The Netherlands, 1981.

(19) Krijn, J.; Baerends, E. J. *Fit Functions in the HFS-method*; Internal report (in Dutch); Free University of Amsterdam: Amsterdam The Netherlands, 1984.

(20) (a) Boerrigter, P. M.; te Velde, G.; Baerends, E. J. *Int. J. Quantum Chem*. **1988**, *33*, 87. (b) te Velde, G.; Baerends, E. J. *J. Comput. Phys*. **1992**, *99*, 84.

(21) Versluis, L.; Ziegler, T *J. Chem. Phys*. **1988**, *88*, 322.

(22) Schlegel, H. B. In *Ab initio Methods in Quantum Chemistry−I*; Lawley, K. P., Ed.; Advances in Chemical Physics Vol. 67; Wiley: New York, 1987.

(23) Vosko, S. H.; Wilk, L.; Nusair, M. *Can. J. Phys*. **1980**, *58*, 1200.

(24) (a) Perdew, J. P.; Chekavry, J. A.; Vosko, S. H.; Jackson, K. A.; Perderson, M. R.; Singh, D. J.; Fioihais, C. *Phys. Rev. B* **1992**, *46*, 6671. (b) Becke, A. D. *J. Chem. Phys*. **1986**, *84*, 4524.

(25) Intramolecular proton transfer from the second shell hydrogen bonding partners and the oxygen ends of the homocitrate ligand did not occur.

(26) Noodleman, L. *J. Chem. Phys*. **1981**, *74*, 5737.

(27) (a) The broken symmetry state is not a pure spin state described by a single determinant, but rather a weighted average of pure spin states. Because the weighting factor of each pure spin state is known, from Clebsch−Gordan algebra, the broken symmetry energy can be expressed in terms of the energies of the pure spin states. For more detail, see ref 26 and references therein. (b) McGrady, J. E.; Stranger, R.; Lovell, T. *J. Phys. Chem. A* **1997**, *101*, 6265.

(28) (a) For the Mo^{4+}4Fe^{2+}3Fe^{3+} and 4Fe^{2+}4Fe^{3+} oxidation states, problems were encountered associated with SCF convergence because of a band of approximately isoenergetic predominantly Fe-based energy levels that give rise to small HOMO−LUMO gaps of ~0.01 eV or less. Here, SCF convergence was achieved by artificially shifting the virtual orbitals to higher energy by 0.3 Hartree. The converged BS wave function and geometry were then used as the starting point for our geometry optimization calculations where this artificial shifting of virtual orbitals was not required. In all cases examined, the geometries and energies for the initial shifted and final unshifted calculations were identical. As a final check that the calculated electronic structure was correct and not an artifact of shifting incorrect virtual orbitals (done at the first SCF cycle and therefore very much dependent on the starting geometry), the Slater transition state method[28b,c] was used to ensure that the correct virtual orbitals were shifted to higher energy. (b) Slater, J. C. *Adv. Quantum Chem*. **1972**, *6*, 1. (c) Slater, J. C. *Quantum theory of molecules and solids*; McGraw-Hill: New York, 1974; Vol. 4.

(29) (a) Mouesca, J.-M.; Noodleman, L.; Case, D. A. *Inorg. Chem*. **1994**, *33*, 4819. (b) Mouesca, J.-M.; Noodleman, L.; Case, D. A.; Lamotte, B. *Inorg. Chem*. **1995**, *34*, 4347.

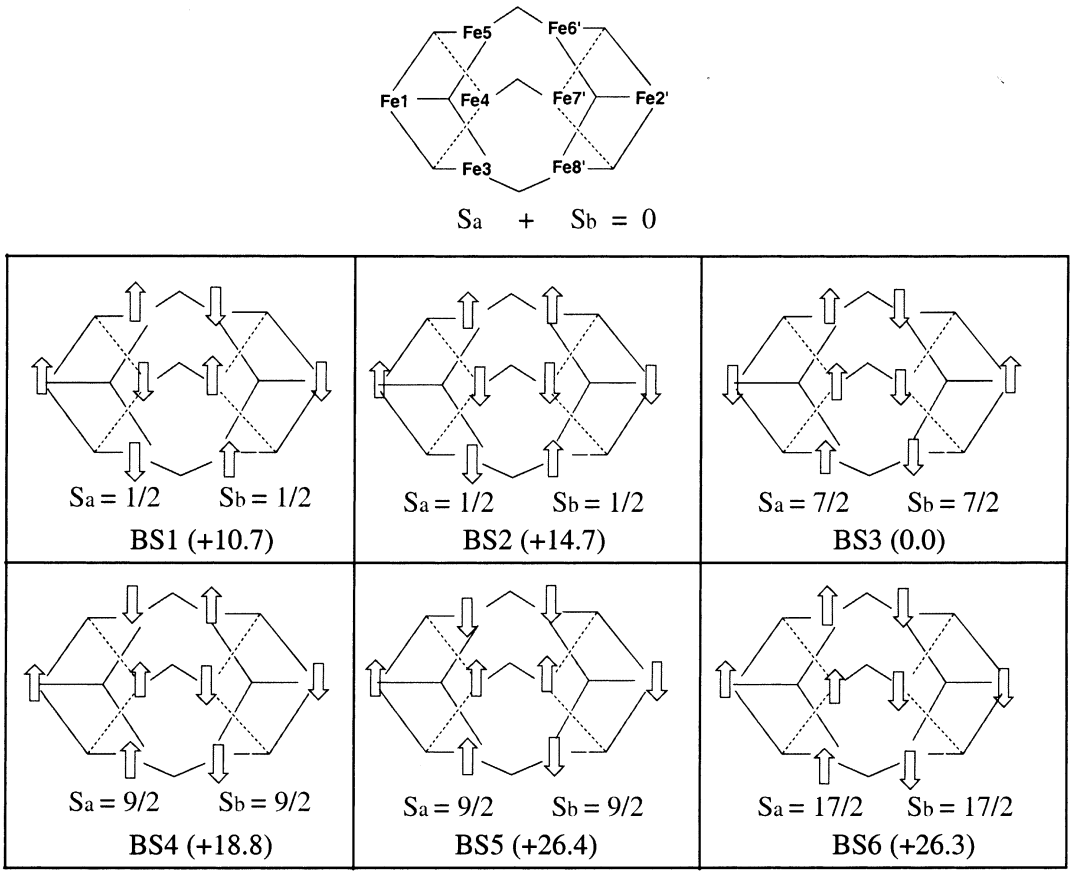

Figure 3. The 6 simple broken-symmetry spin alignment patterns for $6Fe^{2+}2Fe^{3+}$ FeFeco.

thought of as a low-spin Mo^{4+} (d^2) site. By comparison, that the VFe protein displays an $S = {}^3/_2$ EPR signal is also interesting in that no observable V hyperfine interactions have been measured for FeVco.[31] If a V^{2+} (d^3) or V^{4+} (d^1) species were introduced into the cofactor, this would introduce an odd number of electrons at the heterometallic site and hyperfine characteristics on the vanadium ion. It would also require the total spin of the remaining 7Fe system no longer be $S = {}^3/_2$. Given the well-known diagonal relationship in the periodic table and the overall similarities in properties associated with the Mo^{4+} (d^2) and V^{3+} (d^2) ions, the most likely scenario is the direct isoelectronic (in terms of valence electrons) substitution of low-spin Mo^{4+} by low-spin V^{3+}. The proposal of $[V^{3+}Fe^{3+}6Fe^{2+}9S^{2-}]^+$ would give a total electron count of 43 and would not impact upon the spin coupling scheme and the pattern of up and down spin alignments outlined for FeMoco previously. The spin coupling scheme for FeVco should therefore closely follow that of FeMoco, and the most likely BS spin state would be composed of a V3Fe cluster with spin $S_a = 2$ antiferromagnetically coupled to a 4Fe′ cluster with spin $S_b = {}^7/_2$.

The resting state of FeFeco is known to be integer spin (assumed to be $S = 0$ in the ground state) and diamagnetic. We have also used the oxidation state assignments of Lee et al. for FeMoco[5] as a starting point for studies on FeFeco. On that basis, the oxidation state assignments in FeFeco would be $2Fe^{3+}6Fe^{2+}$, and the $S = 0$ state arises from the antiferromagnetic coupling of the Fe site spins in the following manner:

$$\begin{aligned} M_s(\text{total}) &= M_s(\text{4Fe cubane}) + M_s(\text{4Fe′ cubane}) \\ &= M_s(\text{Fe}_1 + \text{Fe}_3 + \text{Fe}_4 + \text{Fe}_5) + M_s(\text{Fe}_2' + \text{Fe}_6' + \text{Fe}_7' + \text{Fe}_8') \\ &= (-{}^5/_2 + 2 + 2 + 2) + (+{}^5/_2 - 2 - 2 - 2) \\ &= 0 \end{aligned} \quad (2)$$

This is one of a number of possible spin alignments. All the spin alignments corresponding to the two $M_s(\text{total}) = 0$ values give a 4:4 pattern, that is, 4 Fe sites of majority spin up and 4 Fe sites of majority spin down. If one considers the simplifying assumption that the cluster exhibits an approximate C_3 axis of rotational symmetry, there are 6 simple spin alignment patterns for FeFeco, shown in Figure 3. Removal of the 3-fold symmetry axis can give rise to additional spin isomer states, but in the case of FeMoco, the energies of the spin isomer states were very similar to that of the original parent BS state. The same phenomenon is also present for the spin isomers of FeFeco, and thus, the spin isomerization phenomenon is not considered here.

Gas-Phase Energetics of FeFeco Spin Coupling Alignments. Figure 3 shows the spin coupling alignments and optimized energies of the 6 simple $S = 0$ BS spin states for

(30) Arber, J. M.; Dobson, B. R.; Eady, R. R.; Stevens, P.; Hasnain, S. S.; Garner, C. D.; Smith, B. E. *Nature* **1987**, *325*, 372.
(31) Hales, B. J. Personal Communication.

FeFeco at the $2Fe^{3+}6Fe^{2+}$ level. The BS states are built up assuming antiferromagnetic coupling prevails between the two cubane halves of the cluster, each cubane half having spin S_a (M3Fe where M = Mo,V,Fe) and S_b (4Fe′). States BS1 and BS2 achieve the $S = 0$ total cluster spin via the AF coupling of two spin one-half cubanes ($S_a = S_b = {}^1/_2$), state BS3 from the AF coupling of two spin seven-half cubanes ($S_a = S_b = {}^7/_2$), states BS4 and BS5 from the AF coupling of two spin nine-half cubanes ($S_a = S_b = {}^9/_2$), and state BS6 from the AF coupling of $S_a = S_b = {}^{17}/_2$ cubanes.

State BS3 lies lowest in energy. The other 5 BS states are excited states ranging from 10.7 to 26.4 kcal/mol in energy above BS3. The state in which all the spins on the Fe site are ferromagnetically aligned (high-spin) lies even higher in energy and is not shown. The large energy difference between the high-spin state and BS3 clearly indicates the important role played by antiferromagnetic coupling between Fe sites in the stabilization of the FeFe cofactor. A similar phenomenon has also been noted in the FeMoco.[13] There is a significant energetic advantage given to BS states with an increasing number of AF interactions. BS3 is the only spin alignment that displays 3 AF interactions between the corner Fe sites, Fe_1 and Fe_2', and the trigonal Fe sites of Fe_3, Fe_4 and Fe_5, Fe_6', Fe_7', and Fe_8'. As Fe(III)/Fe(II) AF interaction energies are generally larger than those for Fe(II)/Fe(II) pairs, this phenomenon is likely correlated with ferric character of Fe_1 and Fe_2'. All other states are higher in energy and display fewer AF interactions involving sites Fe_1 and Fe_2'.

At the $4Fe^{3+}4Fe^{2+}$ level, we have also compared the energies of the different spin coupling alignments in Figure 3. An additional BS state (denoted BS7, spin alignment not shown) consistent with the recent Mössbauer analysis[11] in which there are two ferromagnetic and one antiferromagnetic interactions through the central μS^2 atoms of the cluster (derived from BS1) has also been examined in which the antiferromagnetic coupling of the cluster results from two cubane halves having spin $S_a = 0$ (M3Fe where M = Mo, V, Fe) and $S_b = 0$ (4Fe′). The spin coupling alignment from state BS3 is calculated to be lowest in energy at this oxidation level and comprises the antiferromagnetic coupling of two $S = 4$ cubane halves.

Throughout this analysis of the broken symmetry energies, we have made no mention of the relative strengths of the J couplings or J and B couplings through the three sulfide pathways that link the two subclusters. This information is difficult to tease out of the broken-symmetry states, and we have not as yet evaluated the relative magnitude of the possible intra- and intercluster couplings.

3.2. Isomer Shift Correlation. The Mössbauer isomer shift (IS) provides a good marker for both oxidation state and metal ligand covalency, particularly when comparing related systems. From fundamental physical properties, the isomer shift is proportional to the total s electron density at the Mössbauer nucleus[32] (the Fe sites of the nitrogenase cofactors). The measured s density at the nucleus is altered by changes in Fe(3s) and particularly Fe(4s) valence electrons. Using all-electron DFT calculations, we use a previously constructed linear correlation of measured Mössbauer isomer shifts with computed total s electron density for a variety of 1Fe, 2Fe, and 4Fe sulfur complexes to compare calculated isomer shifts of the nitrogenase cofactors with those measured experimentally.[13] Figure 4 shows one of two typical linear correlation plots of observed isomer shifts in synthetic model systems (filled symbols) versus calculated Fe electron density for the computational model systems of the type $Fe(SR)_n$ ($n = 3, 4$; SR = Sphenyl, $(SR)_2$ = S_2-*o*-xylyl) or $Fe_nS_n(SR)_4$ ($n = 2, 4$; R = phenyl). A similar intercept and slope are also obtained when experimental Fe−S protein isomer shifts are used instead of isomer shifts from synthetic model complexes. The standard deviation for these fits varies between 0.05 and 0.06 mm/s, and correlation coefficients vary from $r = -0.94$ to -0.95. Details of the fitting procedure will be reported elsewhere.[33]

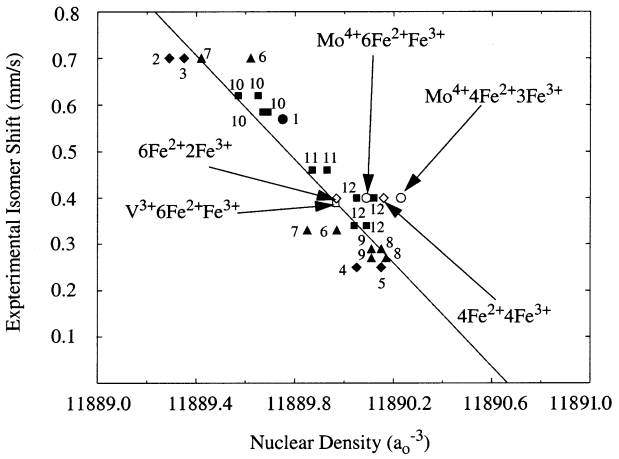

Figure 4. Correlation plot of calculated nuclear density versus observed isomer shift for model Fe−S systems. The plot shown corresponds to isomer shifts derived from a linear fit of 1Fe, 2Fe, and 4Fe S-phenyl and S_2-*o*-xylyl model compounds with available model compound data. Filled symbols correspond to the following: 1, $Fe(SC_6H_5)_3^{1-}$; 2, $Fe(SC_6H_5)_4^{2-}$; 3, $Fe((SCH_2)_2(C_6H_4)_2^{2-}$; 4, $Fe(SC_6H_5)_4^{1-}$; 5, $Fe((SCH_2)_2(C_6H_4)_2^{1-}$; 6, $Fe_2S_2((SCH_2)_2(C_6H_4)_2^{3-}$; 7, $Fe_2S_2(SC_6H_5)_4^{3-}$; 8, $Fe_2S_2((SCH_2)_2(C_6H_4)_2^{2-}$; 9, $Fe_2S_2(SC_5H_5)_4^{2-}$; 10, $Fe_4S_4(SC_5H_5)_4^{3-}$; 11, $Fe_4S_4(SC_5H_5)_4^{2-}$; 12, $Fe_4S_4(SC_5H_5)_4^{1-}$. See text for a detailed discussion.

Average experimental isomer shifts are plotted against the average calculated nuclear densities in Figure 4 for the lowest lying states of FeFeco (BS3) for the $6Fe^{2+}2Fe^{3+}$ and $4Fe^{2+}$-$4Fe^{3+}$ metal-ion valence assignments. Also incorporated in the figure are the valence assignments of $Mo^{4+}6Fe^{2+}1Fe^{3+}$ and $Mo^{4+}4Fe^{2+}3Fe^{3+}$ for FeMoco and $V^{3+}6Fe^{2+}Fe^{3+}$ for FeVco. The $6Fe^{2+}2Fe^{3+}$ point for FeFeco lies much closer to the line of best fit than the $4Fe^{2+}4Fe^{3+}$ alternative. The vertical distance from the open circles to the line for $4Fe^{2+}$-$4Fe^{3+}$ FeFeco (0.10 mm/s) is much larger than for the $6Fe^{2+}$-$2Fe^{3+}$ state. The same trend is apparent for FeMoco in which the more reduced $Mo^{4+}6Fe^{2+}1Fe^{3+}$ oxidation state assignment lies closer to the line of best fit, with errors of around 0.07 mm/s being similar to the error of the monomeric three-

(32) (a) Gutlich, P.; Link, R.; Trautwein, A. *Mössbauer Spectroscopy and Transition Metal Chemistry*; Springer-Verlag: New York, 1978; pp 60−84. (b) Trautwein, A. *J. Phys.* (*Paris*) **1980**, *41*, C1−95. (c) Shirley, D. A. *Rev. Mod. Phys.* **1964**, *36*, 339.

(33) Liu, T.; Lovell, T.; Noodleman, L.; Case, D. A. *Inorg. Chem.*, submitted.

Table 1. Calculated and Experimental ^{57}Fe Isomer Shifts (mm s^{-1}) for FeMoco, FeVco, and FeFeco Clusters

	FeMoco					FeVco			FeFeco				
	$6Fe^{2+}$		$4Fe^{2+}$			$6Fe^{2+}$			$6Fe^{2+}$		$4Fe^{2+}$		
atom	I S[a]	IS[b]	IS[a]	IS[b]	exptl	IS[a]	IS[b]	exptl	IS[a]	IS[b]	IS[a]	IS[b]	exptl
Fe1									0.73	0.68	0.63	0.59	
Fe2	0.37	0.35	0.23	0.22	0.33	0.46	0.43		0.48	0.45	0.32	0.31	
Fe3	0.28	0.27	0.23	0.22	0.51	0.40	0.38		0.36	0.34	0.27	0.26	
Fe4	0.31	0.30	0.25	0.24	0.41	0.35	0.33		0.40	0.38	0.22	0.22	
Fe5	0.21	0.20	0.10	0.10	0.33	0.31	0.30		0.16	0.16	0.04	0.05	
Fe6	0.42	0.40	0.37	0.35	0.39	0.47	0.44		0.45	0.43	0.36	0.34	
Fe7	0.35	0.33	0.28	0.27	0.48	0.42	0.40		0.35	0.33	0.17	0.17	
Fe8	0.34	0.32	0.28	0.27	0.39	0.41	0.39		0.37	0.35	0.32	0.31	
average	0.33	0.31	0.25	0.24	0.40[c]	0.39	0.37	0.39[d]	0.40	0.38	0.29	0.28	0.37[e]/0.42[f]

[a] From linear fit of 1Fe, 2Fe, and 4Fe S-phenyl and S_2-*o*-xylyl group model compounds with available model compound data. [b] From linear fit of 1Fe, 2Fe, and 4Fe S-phenyl and S_2-*o*-xylyl group model compounds with available protein data. [c] Measured at 4.2 K for $S = {}^3/_2$ state from *A. vinelandii* (ref 6). [d] For *A. vinelandii* (ref 10b). [e] For *R. capsulatus* (ref 11). [f] Measured from the subspectral components M_1 and M_2 (ref 11).

coordinate $Fe(SC_6H_5)_3^{1-}$ complex (0.05 mm/s). The corresponding error for the $Mo^{4+}4Fe^{2+}3Fe^{3+}$ oxidation state is much larger (0.15 mm/s). The average isomer shift of the $V^{3+}6Fe^{2+}1Fe^{3+}$ oxidation state for FeVco is shown in Figure 4 to also be in very good agreement with the FeVco experimental isomer shifts.

Table 1 shows the results of applying the two fitting equations to the calculated electron densities at the Fe nuclei in the BS3 state of the FeFeco model cluster. The average calculated IS ($IS_{av} = 0.39$) is close to that observed experimentally ($IS_{av} = 0.40$ mm/s). The calculated isomer shift of $4Fe^{2+}4Fe^{3+}$ is considerably lower ($IS_{av} = 0.29$ mm/s). Overall, these isomer shift estimates, which are very good for FeFeco and FeVco and reasonable for FeMoco, strongly suggest the oxidation state assignments of $6Fe^{2+}2Fe^{3+}$ and $Mo^{4+}6Fe^{2+}Fe^{3+}$ for both FeFeco and FeMoco, respectively, are more compatible with experiment; a more oxidized cluster assignment is not required.

3.3. Optimized Geometries and Fe 3d Net Spin Densities of FeMoco, FeVco, and FeFeco. Optimized geometries of FeMoco, FeVco, and FeFeco (state BS3) are compared in Figure 5. Relevant averaged geometric parameters are listed in Table 2. Net spin populations for the metal sites are also incorporated on the structures in bold type. The geometry of the FeMoco has been discussed in depth elsewhere,[13] and only features important for the comparison with FeVco and FeFeco are recounted here.

For FeMoco, the optimized Mo−Fe, Fe−Fe, and Fe′-Fe′ bond lengths differ from the X-ray structure mainly in the intra-cubane Mo−Fe, Fe−Fe, Fe′-Fe′, and Fe−S distances, with differences no greater than 0.09 Å. Slightly larger deviations are observed for Mo−S, Mo−O, Mo−N, and inter-cubane Fe−Fe′ distances. The space across the central waist of the FeMo cofactor, at $Fe-Fe'_{av} = 2.75$ Å, is also larger than that in the best-resolved crystal structure.[16i] Potential electrostatic effects of nearby positively charged residues (omitted from our model) were noted previously as a possible electrostatic driving force that could shift the bridging μS^2 atoms toward the Arg side chains in the protein, leading to a decrease in the Fe−μS^2−Fe′ angles and an overall shortening of $Fe-Fe'_{av}$.

The calculated geometry of FeVco appears consistent with the FeVco EXAFS data[9,30] in terms of the major V−Fe, Fe−Fe, Fe−S, and V−O/N distances. Comparing the calculated FeMoco and FeVco structure, the replacement of Mo^{4+} by V^{3+} in the cofactor results in a number of structural effects, including a general lengthways expansion of the cofactor from 7.27 to 7.62 Å. The total charge on the cofactor changes from −4 for FeMoco to −5 for FeVco. Relative to FeMoco, the overall expansion can therefore be correlated with the larger electron−electron repulsion spread over the cofactor. The geometries of the 4Fe′ cubanes in both cofactors appear insensitive to the change in total charge of the cofactor; longer calculated VFe distances (2.91 Å, Table 2) result compared to calculated MoFe distances (2.78 Å) in the M3Fe cubane. $Fe-Fe'_{av}$ distances and Fe−μS^2−Fe′ angles are also noted to increase in the V congener, as is suggested by the EXAFS measurements.

The calculated net spin densities are very similarly distributed over the metal atoms in FeMoco and FeVco. In FeMoco, the Mo spin density is calculated to be low and is consistent with the small (but not zero) Mo ENDOR hyperfine signals.[5] The calculated V spin density in FeVco is also similarly small. As there is no observable V hyperfine in the EPR, the spin density on the V atom must also be very small (as V has a large magnetogyric ratio). ENDOR studies may provide additional information on the vanadium oxidation state and spin density but are made more complicated by the fact that the relaxation properties of the VFe protein, derived from the FeVco signal, are unfavorable. This precludes a valuable ENDOR analysis at the present time.[31]

The K-edge EXAFS data[11] for the FeFeco provide strong evidence that the principal structural elements of the FeMoco and FeVco also prevail in FeFeco. Compared to its FeMoco and FeVco analogues, the calculated M−Fe, Fe−Fe′, ∠M−μS^2−Fe, and ∠Fe−μS^2−Fe′ parameters are slightly larger. The Fe^{3+} 3d orbitals are contracted relative to the Mo^{4+} 4d and V^{3+} 3d orbitals, and consequently, orbital overlap between the six-coordinate ferric and the ferrous ions is reduced compared to that in FeMoco. Upon comparing the M−3Fe subcluster of FeMoco and FeFeco, longer Fe−3Fe distances are observed with the Fe−μS^2−Fe angles opening up, and an overall expansion in the Fe−3Fe cubane results. The expansion of the FeFeco is also evident in the average inter-cubane Fe−Fe′ distances (2.89 Å) compared to FeMoco (2.75 Å). As the Fe−μS^2 and Fe′−μS^2 distances are almost

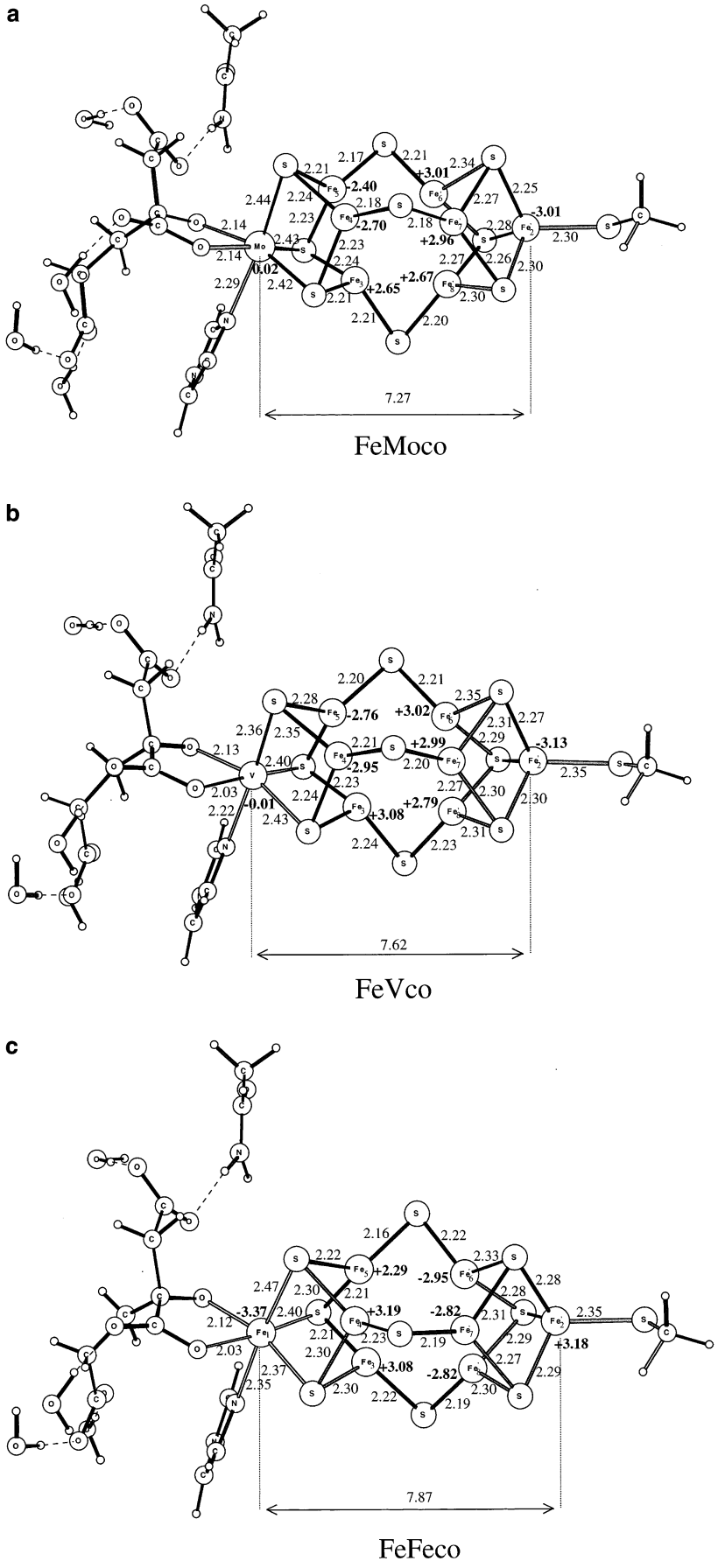

Figure 5. Optimized geometries of $Mo^{4+}6Fe^{2+}Fe^{3+}$ FeMoco, $V^{3+}6Fe^{2+}Fe^{3+}$ FeVco, and $6Fe^{2+}2Fe^{3+}$ FeFeco. Net spin densities are given in bold.

Table 2. Comparison of Selected Calculated and Reported Experimental Parameters (Å and deg) Averaged over the Same Bond Type for $Mo^{4+}6Fe^{2+}Fe^{3+}$ FeMoco, $V^{3+}6Fe^{2+}Fe^{3+}$ FeVco, and $6Fe^{2+}2Fe^{3+}$ FeFeco

	FeMoco[a]			FeVco		FeFeco	
	calcd	EXAFS[b]	exptl[c]	calcd	EXAFS[d]	calcd[e]	EXAFS[f]
M−Fe	2.75	2.68	2.69	2.91	2.76	2.82	2.63
Fe−Fe	2.70	2.62	2.64	2.60	2.65	2.62	2.63
Fe−Fe′	2.75	2.62	2.61	2.88	2.65	2.89	2.63
Fe′−Fe′	2.70	2.62	2.67	2.66	2.65	2.65	2.63
M−S	2.42	2.36	2.32	2.40	2.32	2.41	2.29
Fe−S^2	2.19	2.32	2.21	2.22	2.24	2.21	2.29
Fe−S^3	2.23	2.32	2.24	2.23	2.24	2.26	2.29
Fe′−S^2	2.19	2.32	2.21	2.22	2.24	2.20	2.29
Fe′−S^3	2.24	2.32	2.24	2.23	2.24	2.30	2.29
M−O/N	2.21	2.17	2.40	2.19	2.15	2.17	2.16
∠Fe−μS^2−Fe′	77.6		71.5	81.6		81.8	
∠Mo−μS^3−Fe	74.4		71.8	77.5		81.5	
∠Fe−μS^3−Fe	71.3		71.3	72.7		73.3	

[a] State BS6-1, see reference 13 for a detailed discussion. [b] Reference 35. [c] *Klebsiella pneumoniae*, 1.6 Å resolution, pdb code 1QGU(red). [d] References 9 and 30. [e] State BS3 of this work. [f] Reference 11.

identical to those observed for FeMoco and FeVco, the source of the Fe−Fe′ expansion is traced to the opening up of the Fe−μS^2−Fe′ angle.

AF coupling dominates the spin coupling scheme of FeFeco, particularly across the trigonal ion sites spanning the central cavity of the cluster. Generally, short Fe−Fe interactions (around 2.60 Å or less) occur for pairs of ferromagnetically coupled Fe^{2+} sites where a delocalized minority spin σ electron pathway exists as seen in FeMoco state BS6.[13] When a single site spin vector for one of a ferromagnetic pair of Fe centers is flipped, antiferromagnetic coupling prevails between the two sites (as in FeFeco state BS3), and the pathway for σ electron delocalization is removed. The Fe sites move farther apart to give a much elongated cofactor structure.

The BS3 spin coupling pattern that occurs for FeFeco has a clear effect on the magnitude of the spin densities for the Fe sites. Calculated spin densities of −3.37 at Fe_1 and +3.18 at Fe_2' indicate that high-spin Fe^{3+} sites occupy the six-coordinate and four-coordinate positions with their site spin vectors oppositely aligned. This feature of the electronic structure is consistent with the notion that an even number of ferric and ferrous sites is required to satisfy the diamagnetic $S = 0$ spin criterion of the cofactor.

One final point concerns the elongation of FeFeco along the 3-fold axis as a function for the different spin coupling patterns shown in Figure 3. In Figure 5, if the distance from the six-coordinate metal to the four-coordinate Fe site is taken as an indicator, FeFeco (7.87 Å) is calculated to be significantly longer than either FeMoco (7.27 Å) or FeVco (7.62 Å). The same distance for the different spin alignments of FeFeco are BS1 (7.61 Å), BS2 (7.41 Å), BS4 (7.50 Å), BS5 (7.40 Å), and BS6 (8.29 Å). The majority of these distances are shorter than BS3 (7.87 Å) and fall more in line with those noted for FeMoco and FeVco. These alternative BS states for FeFeco lie too high in energy to be considered as ground states from the simple gas-phase calculations. Additional energetic studies of these alternative BS states are planned when the FeFe protein structure is solved.

4. Conclusions

Biochemical, spectroscopic, and genetics experiments have long pointed toward the existence of structurally homologous cofactors in alternative nitrogenases.[7] As indicated by the experimental results, the cofactors of the conventional (Mo) and alternative (V and Fe) nitrogenase systems are expected to be structurally very similar. The postulated structural homology has relied heavily on spectroscopy and topological analogy with the guiding structure of the FeMoco. As no protein X-ray data containing the alternative cofactors are available to substantiate the structural hypotheses, no absolute structural comparisons to FeMoco have been made. To assess the structural consequences associated with replacement of molybdenum in the FeMoco with V and Fe, spin-polarized BS-DFT calculations have been used to examine the resulting cofactor structures. The introduction of an eighth Fe site into the cofactor template modifies the spin coupling pattern from that found in FeMoco and FeVco. Possible spin coupling alignments and oxidation states for the resting FeFeco having formal metal-ion valencies of $4Fe^{2+}4Fe^{3+}$ and $6Fe^{2+}2Fe^{3+}$ have been examined.

Of the 6 different $S = 0$ spin coupling alignments for FeFeco (Figure 3), the BS3 state spin alignment is preferred on the basis of energetic considerations. At the $6Fe^{2+}2Fe^{3+}$ oxidation level, this BS3 state is composed of a 4Fe cluster with spin $S_a = {}^7/_2$ AF coupled to a 4Fe′ cluster with spin $S_b = {}^7/_2$. This oxidation state is similar to the oxidized state (P^{OX}) of the 8Fe P-cluster in the MoFe protein[34,29a] in that the metal-ion valencies in P^{OX} are $6Fe^{2+}2Fe^{3+}$, that is, two $3Fe^{2+}1Fe^{3+}$ subclusters. The total spin of $S = 4$ for P^{OX} arises from the ferromagnetic coupling of the two cubane halves having spins $S_1 = {}^1/_2$ and $S_2 = {}^7/_2$. The S_2 cubane of P^{OX} is therefore analogous to the S_a and S_b cubanes of FeFeco in terms of oxidation state and spin alignment ($S_2 = S_a = S_b = {}^7/_2$). An identical spin coupling alignment is also lowest in energy at the $4Fe^{2+}4Fe^{3+}$ oxidation level, and the antiferromagnetic coupling of two $S = 4$ cubanes results in the integer spin ground state that is consistent with the observed diamagnetism. However, analysis of the Mössbauer isomer shifts for the more reduced cofactor structures favors M^{n+}-$6Fe^{2+}2Fe^{3+}$ (M = Mo, V, Fe; $n = 3, 4$) as the likely oxidation state assignment for resting FeFeco. When the two electron more oxidized state is constructed, Mössbauer isomer shift values are calculated to be in poorer agreement with experiment.

(34) (a) Zimmermann, R.; Münck, E.; Brill, W. J.; Shah, V. K.; Henzyl, M. T.; Rawlings, J.; Orme-Johnson, W. H. *Biochim. Biophys. Acta* **1978**, *537*, 185. (b) Surerus, K. K.; Hendrich, M. P.; Christie, P. D.; Rottgardt, D.; Orme-Johnson, W. H.; Münck, E. *J. Am. Chem. Soc.* **1992**, *114*, 8579.

(35) (a) Christiansen, J.; Tittsworth, R. J.; Hales, B. J.; Cramer, S. P. *J. Am. Chem. Soc.* **1995**, *117*, 10017. (b) Chen, J.; Christiansen, J.; Tittsworth, R. J.; Hales, B. J.; George, S. J.; Coucouvanis, D.; Cramer, S. P. *J. Am. Chem. Soc.* **1993**, *115*, 5509. (c) Liu, H. I.; Filipponi, A.; Gavini, N.; Burgess, B. K.; Hedman, B.; Di Cicco, A.; Natoli, C. R.; Hodgson, K. O. *J. Am. Chem. Soc.* **1994**, *116*, 2418.

(36) Einsle, O.; Tezcan, F. A.; Andrade, S. L. A.; Schmid, B.; Yoshida, M.; Howard, J. B.; Rees, D. C. *Science* **2002**, *297*, 1696.

The novel cofactor structures appear stable to replacement of the molybdenum by vanadium and iron atoms. In the absence of the availability of the protein environments for the FeVco and FeFeco, one can say little about possible energetic and geometric effects of the protein and solvent environment on the cofactor structures. Nonetheless, in gas phase, there is an expansion of the cofactor structures on progression from FeMoco to FeVco to FeFeco. The calculated structure of the FeFeco displays the largest dimensions of the three cofactors, thus supporting the spectroscopic observation that FeFeco may be the largest member of a family of structurally homologous cofactors found in naturally occurring iron−sulfur proteins.

Acknowledgment. This work was supported by a NIH grant to D.A.C. and L.N. (GM 39914). We thank Brian Hales, Eckard Münck, and Per Siegbahn for useful discussions. We also thank E. J. Baerends and the Amsterdam group for use of the ADF codes.

Note Added in Proof: For the MoFe protein, data analysis of a recent 1.16 Å resolution structure indicates that a ligand (most likely nitrogen) is present at the center of the FeMoco prismane.[36] The question remains whether a similar central ligand occurs in the FeVco and FeFeco structures, and in all cases, what the effects of this additional atom are on geometries, electronic structures, oxidation and spin states.

IC020474U